



Explosive mud volcano eruptions and rafting of mud breccia blocks

Adriano Mazzini^{a,d,*}, Grigorii Akhmanov^b, Michael Manga^c, Alessandra Sciarra^d,
Ayten Huseynova^e, Arif Huseynov^e, Ibrahim Guliyev^e



^a Centre for Earth Evolution and Dynamics (CEED), University of Oslo, Oslo, Norway

^b Faculty of Geology, Lomonosov Moscow State University, Moscow, Russian Federation

^c Department of Earth and Planetary Science, University of California, Berkeley, USA

^d Istituto Nazionale di Geofisica e Vulcanologia (INGV), Sezione Roma 1, Italy

^e Oil and Gas Institute, Azerbaijan National Academy of Sciences, Baku, Azerbaijan

ARTICLE INFO

Article history:

Received 6 June 2020

Received in revised form 11 October 2020

Accepted 26 November 2020

Available online xxxx

Editor: J.-P. Avouac

Keywords:

Lokbatan mud volcano Azerbaijan

rafted mud breccia megablocks

gas flux

self-sealing

explosive eruptions

lubrication theory

ABSTRACT

Azerbaijan hosts the highest density of subaerial mud volcanoes on Earth. The morphologies characterizing these structures vary depending on their geological setting, frequency of eruption, and transport processes during the eruptions. Lokbatan is possibly the most active mud volcano on Earth exhibiting impressive bursting events every ~ 5 years. These manifest with impressive gas flares that may reach more than 100 meters in height and the bursting of thousands of m^3 of mud breccia resulting in spectacular mud flows that extend for more than 1.5 kilometres. Unlike other active mud volcanoes, to our knowledge Lokbatan never featured any visual evidence of enduring diffuse degassing (e.g., active pools and gryphons) at and near the central crater. Only a very small new-born gryphon was intermittently active in 2019 (with negligible flow). Gas flux measurements completed with a closed-chamber technique reveal extremely low values throughout the structure with average $\text{CH}_4 = 1.36 \text{ tonnes yr}^{-1}$ and $\text{CO}_2 = 11.85 \text{ tonnes yr}^{-1}$. We suggest that after eruptive events, the mud breccia is able to seal the structure preventing gas release and thereby promoting overpressure build-up in the subsurface. This self-sealing mechanism allows a fast recharge of Lokbatan resulting in more frequent and powerful explosive episodes. Our field observations reveal the presence of large (up to $\sim 50,000 \text{ m}^3$) stratified blocks that were originally part of a large crater cone. These blocks were rafted $> 1 \text{ km}$ from the vent on top of mud breccia flows. We use a model based on lubrication theory to show that it is reasonable to transport blocks this large and this far provided the underlying mud flow was thick enough and the blocks are large enough. The presence of large rafted blocks is not a unique phenomenon observed at Lokbatan mud volcano and is documented at other large-scale structures both onshore and offshore.

© 2020 The Author(s). Published by Elsevier B.V. This is an open access article under the CC BY license (<http://creativecommons.org/licenses/by/4.0/>).

1. Introduction

Mud volcanism is a geological phenomenon whose spectacular activity is driven by a combination of the gravitative instability (e.g., shale buoyancy and density inversion) of the more buoyant rapidly buried sediments, and by the overpressure resulting from the generation of hydrocarbons at depth (Mazzini and Etiope, 2017). Mud volcanoes (MVs) are distributed worldwide in sedimentary basins in active and passive tectonic settings (Aliyev et al., 2015). The highest MV density on Earth is in the Caspian region, and in particular in Azerbaijan, where hundreds of structures

are distributed both offshore and onshore (Jakubov et al., 1971). The largest variety of morphological types of MVs are also found in this so-called “land of fire”. Individual structures may reach diameters of several kilometres and heights up to 600 m. Many of these structures alternate between periods of dormancy and vigorous eruption.

Lokbatan MV is the structure with the greatest number of known eruptions, most of which display spectacular explosive events. The first recorded eruption occurred on the 6th January 1829 (Aliyev et al., 2002). Intervals between eruptions are typically ~ 5 years. Nearly 25 major explosive events have been documented during the past century (Aliyev et al., 2002; Mazzini and Etiope, 2017). The mechanisms that control such intense eruptive activity remain unclear. Lokbatan MV (Fig. 1A) is situated in the Absheron region ($\sim 15 \text{ km}$ SW from Baku) along the crest of Lokbatan anticline. The axis of this structure continues towards the

* Corresponding author at: Centre for Earth Evolution and Dynamics (CEED), University of Oslo, Oslo, Norway.

E-mail address: adriano.mazzini@geo.uio.no (A. Mazzini).

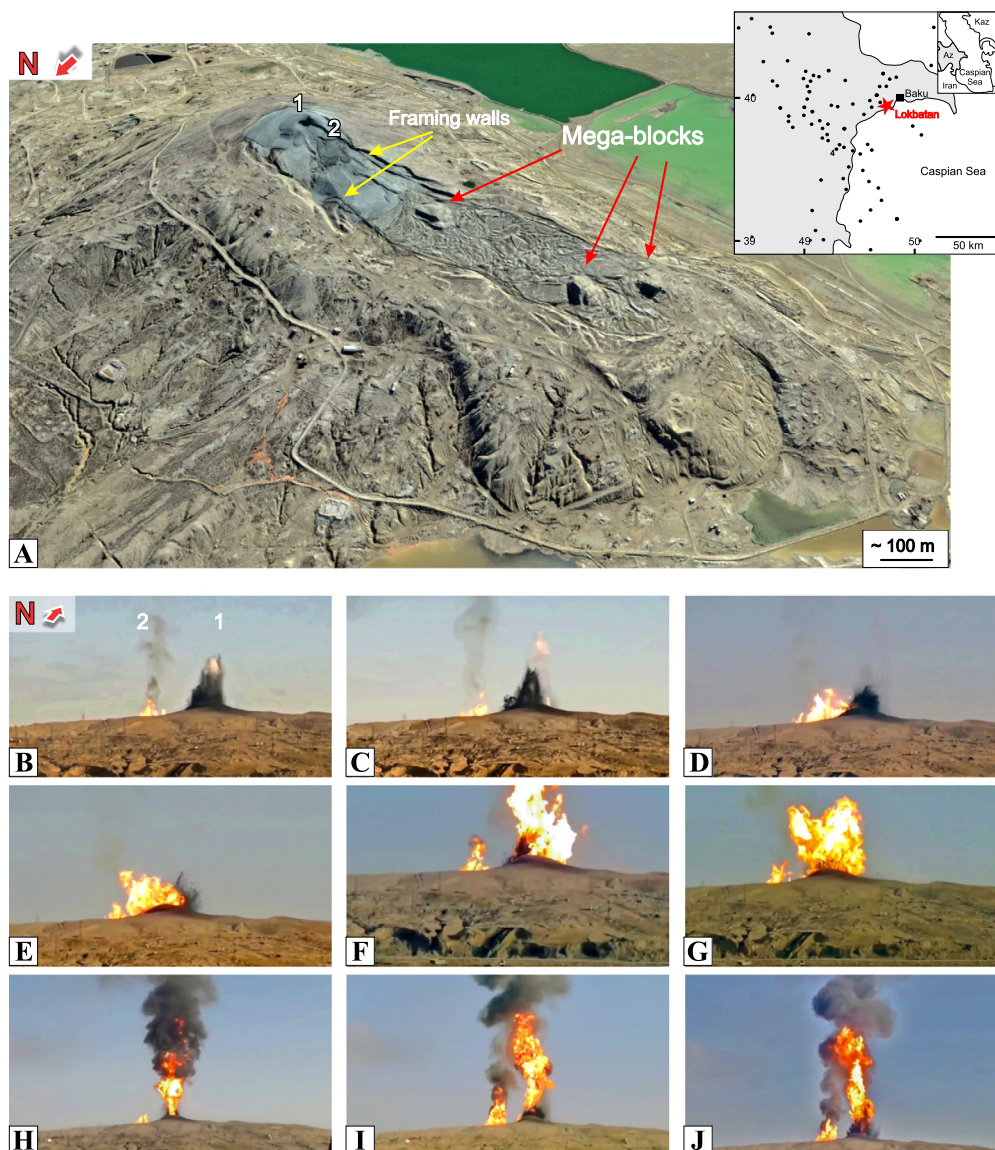


Fig. 1. Lokbatan morphology and eruptions. (A) Google Earth image of Lokbatan MV and flows (May 23, 2019, 3× vertical exaggeration). Indicated by red arrows (interpreted rafted fragments of older cones); numbers indicate the younger crater (2) that formed during the 2012 eruption and an older crater (1) that was also reactivated during the 2012 event. Inset map shows location of other mud volcanoes (black dots) including Lokbatan (red star symbol). (B–K) Various phases of the 20th September 2012 Lokbatan eruption when two craters (indicated accordingly as 1 and 2) were simultaneously active. (B–D) methane released from crater 2 (in the background) is ignited, while crater 1 (on the foreground) erupts mud breccia to the surface by powerful surges of methane (white cloudy area in B–C). (E–G) Flames extend to crater 1 igniting methane and mud breccia. (H–J) Burning of oil and methane resulting in tall black flames. (Sumgait, 2016, January 5). (For interpretation of the colours in the figure(s), the reader is referred to the web version of this article.)

west and curves towards the NW hosting also other active MVs (e.g., Akhtarma-Putu, Kushkhana, Shongar, Saryncha). Regional tectonic structures are suggested to constrain the elongated shape of Lokbatan MV and its main flows (Planke et al., 2006; Bonini, 2012).

Planke et al. (2006) interpret this geometry as a graben structure related to the collapse of an elongated subsurface mud chamber. The authors also describe the large isolated blocks on the western mud breccia flow as horsts. Roberts et al. (2011) relate the same megablocks to debris avalanche deposits. So far it remains unknown if these so called “horsts” or “megablocks”, are tectonically formed, are related to gravitative mass transport processes, or have a local origin through mud volcanism.

The goals of this study are to investigate the dynamics and driving mechanism of the frequent and powerful eruptions of Lokbatan MV. Field measurements and observations are used to introduce

a conceptual and mechanical model for megablock transport processes in the mud flows.

2. Methods

We visited Lokbatan MV during several field expeditions and in particular during 2005, 2006, 2018 and 2019 to map and characterize structures at the site. The latest field expeditions are part of the Azerbaijan Summer School Program, organized in the framework of the HOTMUD project. Field observations and measurements at the crater site and along the mud breccia flows are combined with satellite images to constrain the model for block transport.

In addition, 30 CO₂ and CH₄ flux stations were completed throughout a large area of Lokbatan MV using a West System™ speed-portable “closed dynamic” accumulation chamber “time zero” instrument (e.g. Cardellini et al., 2003a). The device is equipped

with two infrared spectrophotometer detectors. The CO₂ detector is a Licor LI-820 able to measure from 0 up to 26400 g m⁻² d⁻¹. This detector is a double beam infrared CO₂ sensor compensated for atmospheric temperature and pressure. Accuracy of the concentration reading is 2% and repeatability is ±5 ppmv. The CH₄ flux meter is TDLAS (Tunable Diode Laser Absorption Spectroscopy) with multipass cell (West System assembled CH₄ sensor) with 10000 ppmv full scale value that allows the measurement of flux in the range from 8 up to 24000 mg m⁻² d⁻¹. The accuracy of the concentration reading is 0.1 ppmv, and the lower detection limit is 0.1 ppmv. The recorded concentrations measured over time, with other parameters such as volume and surface of the accumulation chamber, allow us to calculate the exhalation flux from soil (e.g. Hutchinson et al., 2000).

The probability distribution analysis of flux data was performed through the statistical approach of Sinclair (1974, 1991). This method is used in order to establish statistical population classes for each parameter on the basis of gaps and/or slope changes in the linear normal distribution. The identification of different population classes allowed us to choose contour thresholds distinguishing between an upper or anomalous data set and a lower set. The natural neighbour interpolation between individual gas measurements (Sibson, 1981) was applied in order to create the maps for CO₂ and CH₄ diffuse degassing, according to the population classes recognised by Normal Probability Plot (NPP) elaboration. Estimates of the total CO₂ and CH₄ output were determined according to the Chiodini and Frondini (2001) approach.

3. Results

3.1. Field observations

The most recent Lokbatan eruption started at 7:55 am on the 2nd of May 2017 and the most intense activity lasted for about 4 minutes. The area covered by mud breccia during this eruption extended over a region of 0.7 ha. During this event, the Republic Seismic Survey Center of Azerbaijan National Academy of Sciences recorded earthquakes from a depth of ~4 km. One of the most spectacular eruptions occurred on the 20th September 2012 (Aliyev et al., 2015) during which a 100 m tall fire column blasted into the air with a copious amount (estimated up to 300,000 m³) of mud breccia (Fig. 1B–J). During this event, a second distinct crater formed ~60 m to the west of the main vent (Figs. 1–2). The volcano has an elongated shape that coincides with the direction of numerous superposed mud breccia flows that in turn follow the anticline axis hosting the structure. The mud breccia consists of a silty-clayey matrix incorporating numerous differently sized (from a few cm to ~0.5 m) angular fragments of well-lithified sandstones, mudstones and siderite concretions. Among the largest specimens, we observed sandstone blocks larger than 1 m³ in volume. These characteristics are observed throughout the MV edifice and this mud breccia lithology is present over an area of ~5 km². The main flows form a long tongue that extends from the main and secondary craters towards the west for nearly 2 km forming a triangular-shaped morphology (Fig. 1A). In fact, this flow tongue widens from ~30 m around the crater up to 500 m in the more distal regions. The tongue dissects the MV on its western flank forming a depression whose borders are clearly defined by framing E-W oriented sub-vertical walls. These walls are ~8 m high in the flow portion closer to the crater and are not visible in the most distal parts of the westernmost side of the mud breccia tongue (Fig. 2E). The central and distal parts of the flow preserve at least three large (ranging in size from 0.3 to 0.7 ha) and tall (up to 20 m) blocks distributed between 500 m and up to 1 km from the main crater (Figs. 1–2). One side of some of these enigmatic features is characterized by sub vertical walls and by a gentler slope

on the other flank (Fig. 2B–D). The base of the walls is covered by a debris fall talus due to extensive weathering of poorly lithified/loose sediments (Fig. 3A). These walls reveal important details about the internal structure of these blocks. They consist of distinct units of overlapped mud breccia flows (thicknesses ranging from 1 to 4 m, Fig. 3B) intersected by perpendicular fractures that resemble columnar joints (Fig. 3C). The same patterns are also clearly visible in the mud breccia outflows from the crater site (Fig. 3D). These vertically-oriented “columnar jointing” structures witnessed the rapid degassing and desiccation of the fluid-rich mud breccia after the eruptions and are typical at many MV sites. It is important to note that in the studied blocks, the mud breccia layers and fractures normal to the block surface have variable inclinations (up to ~35°, depending on the block). This implies that these megablocks were tilted from their original sub-horizontal orientation. We suggest that these blocks represent portions of the western rim of the main crater that breached during one of the powerful eruptions and were displaced downhill along the mud flow. This also explains the amphitheatre shape of the MV crater edifice with a wide opening towards the west.

3.2. Flux measurements

Despite its frequent and large eruptions, during its dormancy Lokbatan MV does not reveal any evidence of obvious degassing in the region in and around the crater. Only one isolated and very small (~40 cm tall) gryphon recently appeared in the oldest crater. CO₂ and CH₄ diffuse flux measurements were completed over a region of 30,254 m² in order to quantify the ongoing degassing. The main statistics for miniseepage flux data (Table 1) show that CO₂ has a low dispersed distribution, as highlighted by the low value of the standard deviation (4.35), while CH₄ has a high dispersed distribution with a high standard deviation (208.72) and a wide range of values.

The gryphon site reveals the highest focused fluxes (0.498 kg d⁻¹ of CO₂ and 0.310 kg d⁻¹ of CH₄). Excluding this outlier, the remaining measurements range between 0.5–15.5 g m⁻² d⁻¹ for CO₂ and 0.86–637.5 mg m⁻² d⁻¹ for CH₄ (Table 1). The population partitioning method, applied to all the flux measurements, produced a probability plot for the recorded CO₂ values (Fig. 4A). The plot reveals that most of the CO₂ measurements can be ascribed to Group A values (73% of total data) that includes fluxes up to 8 g m⁻² d⁻¹. Group B, which represents 20% of the total data, has an average flux of 12.55 g m⁻² d⁻¹, while Group C is represented by only two stations with an average flux of 17.72 g m⁻² d⁻¹. The CH₄ flux measurements were also divided into three population classes (Fig. 4B): Group A representing 60% of the total data, with a mean flux of 21.58 mg m⁻² d⁻¹ and threshold at 100 mg m⁻² d⁻¹; Group B, representing the 20% of the total data with a mean flux value of 244.11 mg m⁻² d⁻¹; Group C representing the 20% of the total data with a mean flux value of 666.73 mg m⁻² d⁻¹. The maps obtained from the natural neighbour interpolation of the flux measurements (Fig. 4C,D) divided in population classes, show higher degassing in a restricted area surrounding the gryphon and on the southern flank of the main crater (1). Higher flux values are also observed at the recently erupting crater (2) to the west and, with a more prominent anomaly, within a circumscribed region between the two eruption vents. The rest of the structure is characterized by low values for both measured gas species. The study area (30,254 m²) has a calculated total CO₂ output of 11.85 tonnes yr⁻¹ and total CH₄ emission of 1.36 tonnes yr⁻¹ (Table 2).

3.3. Model for rafting blocks

Given the observations that the large blocks appear to be displaced fragments of the main cone, we now develop a model to

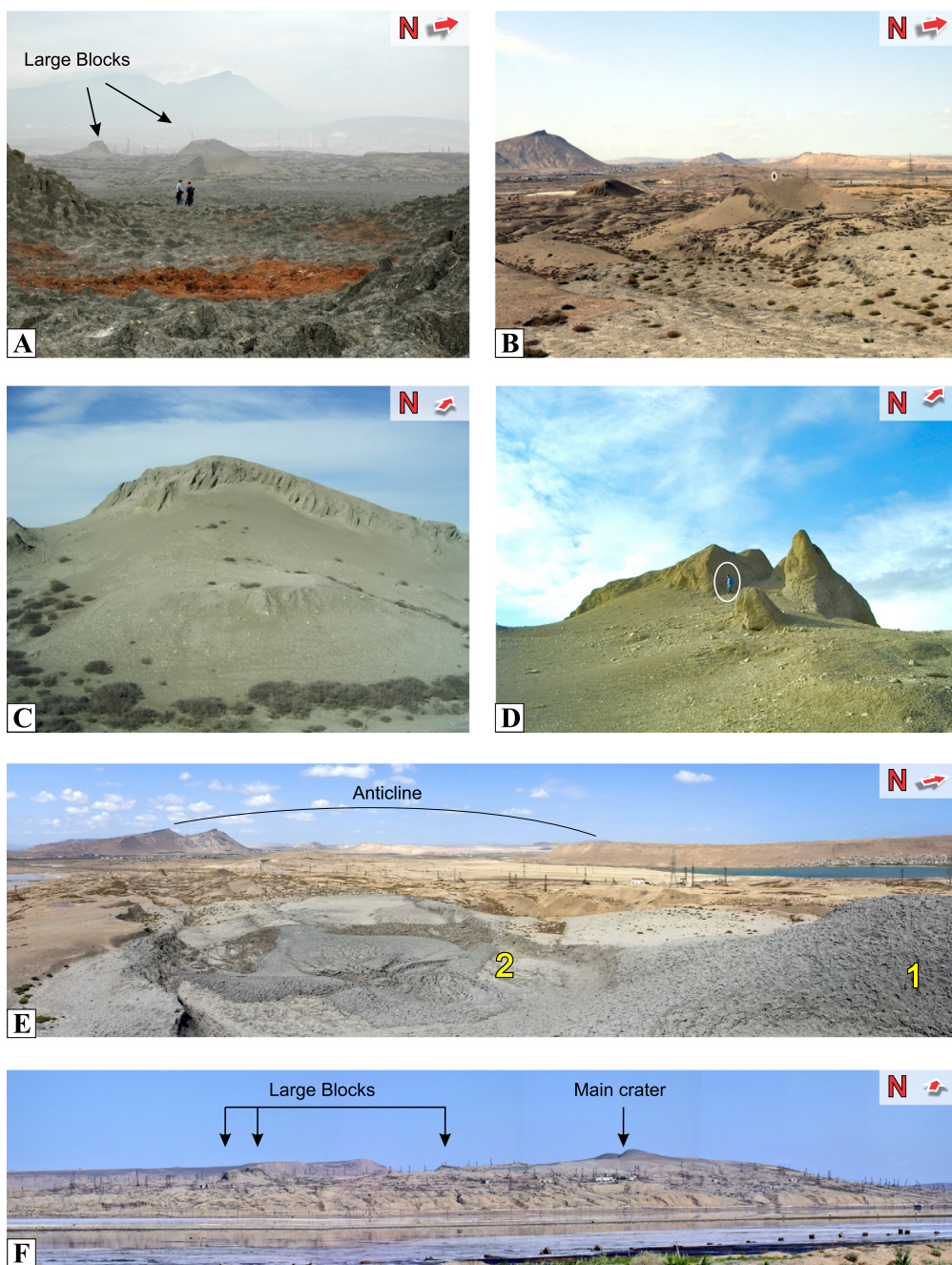


Fig. 2. Field images of the large blocks at Lokbatan MV. (A) October 2005 view from Crater 1 with red coloured mud breccia baked during one of the latest explosive eruptions; in the background are visible the large blocks (arrows). (B–D) Large blocks with subvertical walls (circled people for scale). (E) View of the long mud breccia flow from crater 1. The second crater is indicated (2) and the large blocks are visible. The eroded anticline is also indicated. Note the numerous wells surrounding the mud volcano. (F) Side view of the MV, the main crater (1) area reaches a height of ~110 m. Indicated are also the blocks emerging from the lateral flow. Note the dozens of oil wells surrounding the MV.

Table 1

Main statistical parameters of measured CH₄ and CO₂ miniseepage (i.e. excluding the gryphon) flux data from Lokbatan MV compared to world averages on microseepages¹ (Etiopie et al., 2019) and to miniseepage from Nirano MV² (Sciarrà et al., 2019).

	Mean	Geometric mean	Median	Min	Max	Lower value	Upper value	Std. dev.
			ϕCH_4 (mg m ⁻² d ⁻¹)					
Lokbatan	133.76	33.65	26.31	0.86	637.48	8.78	189.73	208.72
World average microseepages ¹	194.8	4.02	2.73	0.01	7087.7	–	–	711.1
Nirano MV ²	220.9	–	0.01	0.01	3208.5	0.003	0.028	2547.5
			ϕCO_2 (g m ⁻² d ⁻¹)					
Lokbatan	4.53	3.06	2.53	0.54	15.46	1.70	5.86	4.35
Nirano MV ²	17.9	–	16.68	0	91.41	9.33	22.7	12.9



Fig. 3. Large blocks and mud breccia flow structures. (A) Overview of the three large blocks within the main Lokbatan mud flow. The debris fall talus is visible at the foot of the walls on the steeper side of some of these blocks. (B) Portion of one of the megablock walls showing distinct mud breccia flow events up to several meters thick. (C) Detail of the same wall showing the layering of the mud breccia flows (mudflow boundaries are indicated by dashed lines). Note that these units display structures similar to columnar jointing that have orientation perpendicular to the layering. (D) Examples of the same structures observed in the area around the crater site characterizing the most recent mud breccia flow. (E) Unique and isolated small gryphon that formed in the main crater (1) in 2019, height ~ 40 cm.

assess whether it is reasonable to transport blocks such large distances. We assume that during one (or more) eruption the western part of the main conical edifice was broken apart. The large blocks from the cone are liberated and mobilized by viscous mud breccia flows (hereafter “fluid”), as illustrated schematically in Fig. 5. The blocks are then carried along with the flow. Buoyancy forces cause the blocks to move both downslope with respect to the underlying fluid and also to sink through that fluid. When the blocks sink far enough they become stuck on the substrate underlying the flow, terminating their rafting.

To quantify the transport of blocks we consider the motion of a single block with density ρ_b over and through a fluid with viscosity μ and density ρ_m and down a surface with slope θ . We consider a two-dimensional geometry allowing the block and surrounding fluid to move both downslope and perpendicular to the ground surface. Geometry and variables are illustrated in Fig. 6: block length and thickness are L and w_0 , respectively, and the thickness of mud under the block is h .

We assume that flow is laminar, with Reynolds number $Re = \rho_m U h / \mu$ less than $\sim 10^3$, reasonable for mud breccia flows (e.g., Menapace et al., 2019) and approximate the mud breccia as a Newtonian fluid. Since motion is nearly unidirectional when $L \gg h$, momentum conservation is governed by Stokes equations. Time dependence does not explicitly enter the equations, but h and w vary over time as the block sinks. The linearity of the gov-

erning equations for mass and momentum conservation allows us to decompose the flow and boundary conditions into 3 separate problems, illustrated in Fig. 6b–d, and then to superimpose the solutions.

For problem 1 (Fig. 6b), velocity $u_1(y)$ is governed by the balance between viscous stresses and buoyancy

$$\mu \frac{d^2 u_1}{dy^2} = \rho_m g \sin \theta \quad (1)$$

with boundary conditions $u = 0$ at $y = 0$ and $du_1/dy = 0$ at $y = h$. The no-slip boundary condition at the bottom of the block is not accounted for in this problem as it addressed in problem 2 (Fig. 6c).

For problem 2 (Fig. 6c), the velocity $u_2(y)$ is obtained by balancing the downslope gravitational force from the block with viscous stresses in the underlying fluid

$$\mu \frac{du_2}{dy} = \rho_b g w \sin \theta + (\rho_b - \rho_m) g (h_0 - h) \sin \theta \quad (2)$$

with boundary conditions $u = 0$ at $y = 0$. U is then given by $u_1(y) + u_2(y)$ evaluated at $y = h$,

$$U = \frac{gh \sin \theta}{2\mu} [2\rho_b w + \rho_m h + 2(\rho_b - \rho_m)(h_0 - h)]. \quad (3)$$

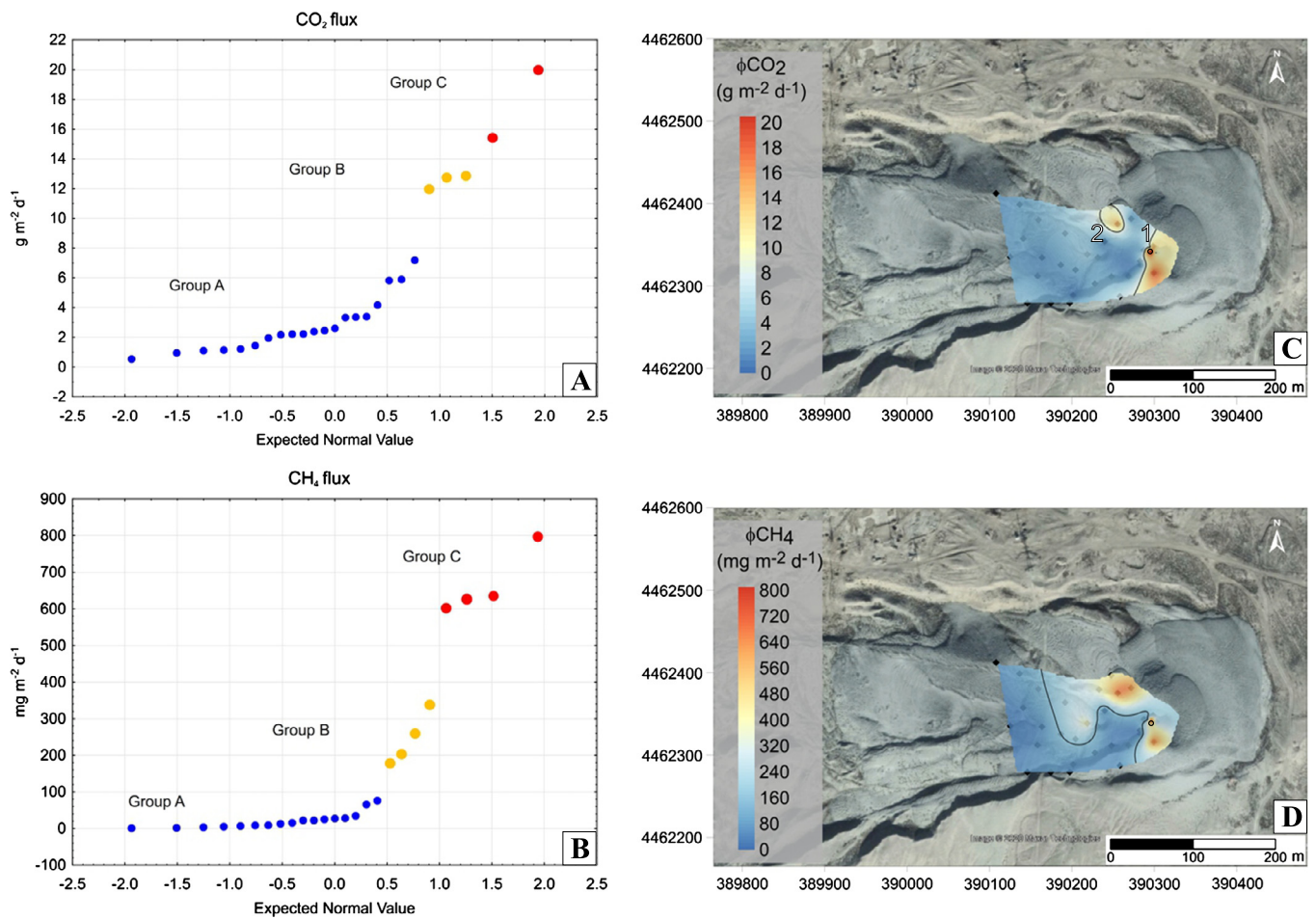


Fig. 4. Flux measurements at Lokbatan MV. (A–B) Normal probability plots for the CO₂ (A) and CH₄ (B) fluxes. (C–D) Spatial distribution of flux measurements for CO₂ and CH₄ respectively. The highest fluxes are recorded at the gryphon site at crater 1 (black-framed circle). Satellite image from arcGis. The black line defines the threshold for values higher than those defined for Group A. Measured stations are indicated by shaded diamonds.

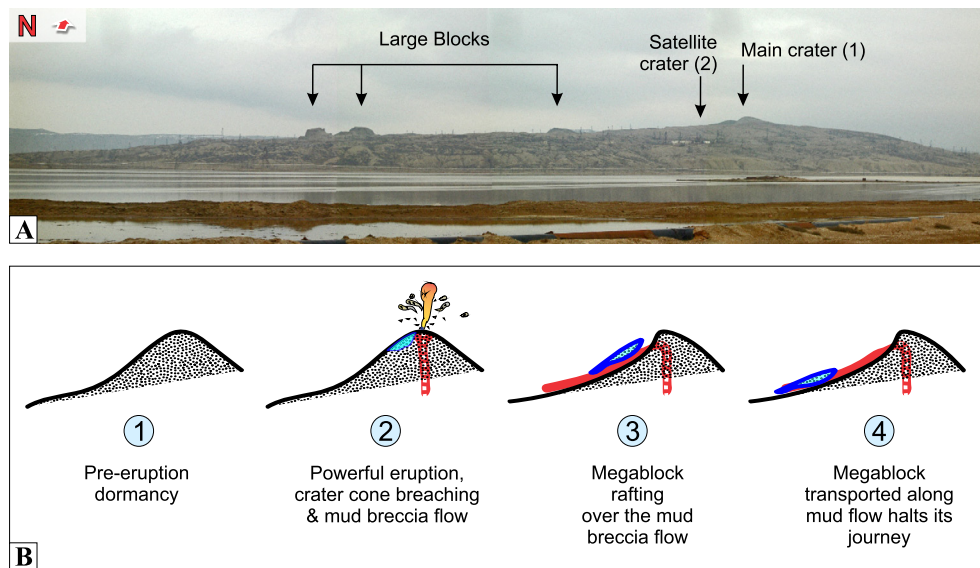


Fig. 5. Megablock transport conceptual model. (A) Panorama view of Lokbatan MV. Indicated are the positions of the main crater and the secondary crater and the megablocks along the mud flow on the western flank of the volcano. (B) Schematic illustration of the different stages that create large blocks and then allow them to be transported, with red indicating the new mud breccia flow and the stippled region showing the pre-existing MV structure.

Table 2

Measured CH₄ and CO₂ flux data from Lokbatan and other mud volcanoes. Etiope et al., 2004b reports a survey done after the October 2001 eruption;[§] indicates measurements close to flames still active after the Oct 2001 eruption.

Country	MV	MV Area (approx. value km ²)	Investigated Area (tonnes km ²)	Mini-seepage (tonnes yr ⁻¹)	Macro-seepage (tonnes yr ⁻¹)	Total emission (tonnes yr ⁻¹)	Emission factor (km ⁻² yr ⁻¹)	References
ϕ_{CH_4}								
Azerbaijan	Lokbatan	5	0.03	1.25	0.11	1.36	45	This study
	Lokbatan	2.98	0.1	8 [§] + 11.2	N.A.	19.2	192	(Etiope et al., 2004b)
	Dashgil	3	0.6	104	623	727	1200	(Etiope et al., 2004b)
	Kechaldag	1	0.05	5.8	4	9.8	196	(Etiope et al., 2004b)
Japan	Bakhar	2.5	0.05	5.5	8.4	14	230	(Etiope et al., 2004b)
	Murono	0.1	0.005	16	5	21	4286	(Etiope et al., 2011)
	Kamou	<0.01	0.001	1.2	1.8	3	3000	(Etiope et al., 2011)
Italy	Maccalube	1.5	1.4	374	20	394	281	(Etiope et al., 2019)
	Regnano	0.1	0.006	29	5	34	5667	(Etiope et al., 2007)
	Frisa	<0.01	0.001	2.8	2	5	4800	(Etiope et al., 2019)
	Pineto	<0.01	0.0025	1.7	1.6	3	1320	(Etiope et al., 2019)
	Serra de Conti	0.01	0.006	12	7	19	3167	(Etiope et al., 2019)
Romania	Nirano	0.2	0.0787	2.13	4.72	6.85	87	(Sciarra et al., 2019)
	Monor	<0.01	0.002	13.9	2.1	16	8000	(Spulber et al., 2010)
	Beciu	0.2	0.005	7.5	182	189	37900	(Frunzeti et al., 2012)
	Paclele Mici	0.5	0.62	128	255	383	618	(Etiope et al., 2004a)
	Paclele Mari	1	1.62	430	300	730	450	(Etiope et al., 2004a)
	Fierbatori	0.7	0.025	20	17	37	1480	(Etiope et al., 2004a)
	Andreiasu		0.000012			1.8		(Baciu et al., 2018)
	Lepsa		0.000012			1.5		(Baciu et al., 2018)
	Lopatari		0.000452			27		(Baciu et al., 2018)
	Raiuti		0.000006			3		(Baciu et al., 2018)
	Alimpesti		0.00018			19		(Baciu et al., 2018)
	Sacelu-Gorj		0.0000004			0.03		(Baciu et al., 2018)
	Taiwan	Wu-shan-ding	<0.2	0.006	30.2	4.8	35	5833
China	Dushanzi	0.4	0.02	20.1	2.5	23	1130	(Zheng et al., 2017)
ϕ_{CO_2}								
	Lokbatan	5	0.03	11.67	0.18	11.85	391.5	This study
	Nirano	0.2	0.0787	299.3	0.14	299.44	3805	(Sciarra et al., 2019)

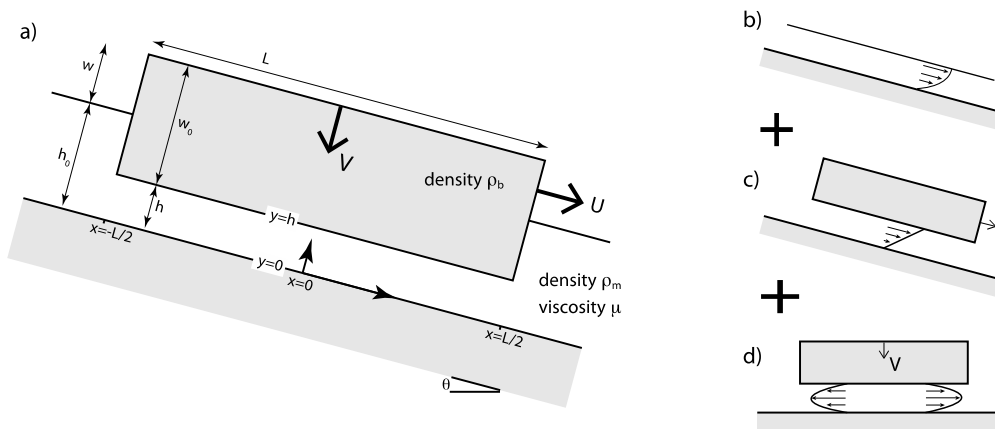


Fig. 6. a) Definition of model geometry, length scales and coordinate system. The solution to this problem is obtained by superimposing solutions for the motion of b) a plane layer of fluid, c) the motion of a block over a plane layer, and d) the squeezing flow or lubrication problem with appropriate boundary conditions.

Problem 3 (Fig. 6d) describes the squeezing flow generated by the sinking of the block, a classic lubrication theory problem governed by the Reynolds equation that relates the downward motion of the block V to the pressure distribution $p(x)$ under the block

$$\frac{d}{dx} \left(\frac{\rho h^3}{12\mu} \frac{dp}{dx} \right) = \rho V, \quad (4)$$

with boundary conditions $p = 0$ at $x = \pm L/2$ and $dp/dx = 0$ at $x = 0$. The pressure distribution is thus

$$p(x) = \frac{6\mu V}{h^3} \left(x^2 - \frac{L^2}{4} \right). \quad (5)$$

To obtain the settling speed V we balance the buoyancy of the block with the upward force from the pressure

$$\int_{-L/2}^{L/2} p(x) dx = gL \cos \theta [\rho_b w + (h_0 - h)(\rho_b - \rho_m)] \quad (6)$$

leading to

$$V = \frac{dh}{dt} = \frac{2g \cos \theta h^3}{\mu L^2} [\rho_b w + (h_0 - h)(\rho_b - \rho_m)]. \quad (7)$$

The ratio of downslope to vertical speeds is thus

$$\frac{U}{V} = \frac{1}{4} \left(\frac{L}{h} \right)^2 \tan \theta \left[\frac{2w + (\rho_m/\rho_b)h + 2[1 - (\rho_m/\rho_b)](h_0 - h)}{w + [1 - (\rho_m/\rho_b)](h_0 - h)} \right] \quad (8)$$

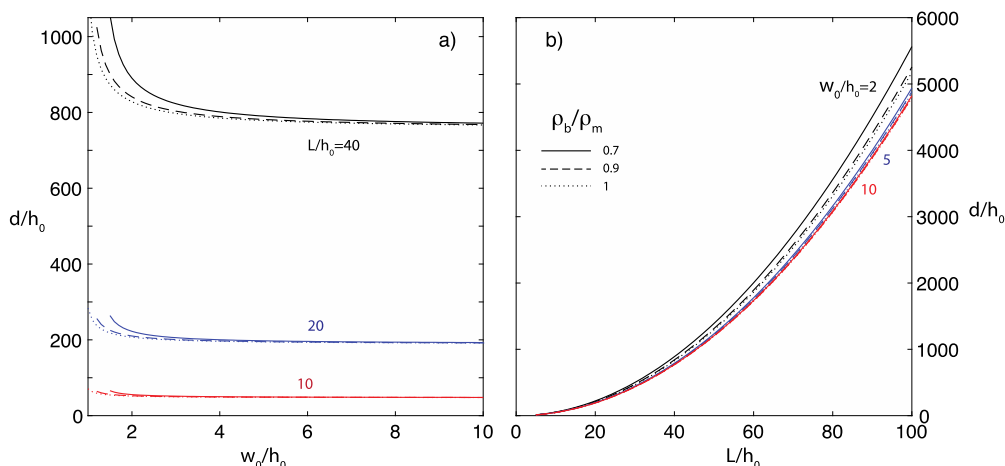


Fig. 7. a) Distance d traveled as a function of block height w_0 for different block lengths L . b) Distance d traveled as a function of block length L for different block heights w_0 . In both panels, all lengths are normalized by initial flow thickness h_0 . Solid, dashed and dotted lines are for ρ_b/ρ_m of 0.7, 0.9 and 1, respectively.

and we note that w and h vary over time, given by $dw/dt = dh/dt = V$.

Because both the downslope and sinking velocities are inversely proportional to viscosity, the distance blocks travel is independent of viscosity. This is true provided the flow is laminar so that equations (1), (2) and (4) apply. Rather, the distance traveled depends most strongly on the lateral dimension of the blocks (equation (8)): large blocks travel further because it is more difficult to squeeze out fluid from the region under the block as L/h increases – thin gaps, $h \ll L$, are the basis for lubrication phenomena.

To illustrate how geometry affects transport, we compute the distance blocks will travel assuming they come to rest when they sink 90% of the way through the underlying fluid, i.e., they reach $h/h_0 = 0.1$. The number 90% is arbitrary but captures the condition that the block has settled most of the way through the flow. We can integrate equation (7) with respect to time, using $w = h - h_0 + w_0$, to find the time it takes for the block to sink a distance $0.9h_0$ and integrate equation (3) for U to determine the distance the block has traveled. Fig. 7A–B shows the distance traveled normalized by the initial thickness, d/h_0 , as a function of the initial block height w_0/h_0 and block length L/h_0 , also normalized by the initial flow thickness. We consider density ratios ρ_b/ρ_m of 1, 0.9 and 0.7. The slope angle is assumed to be 6° – the slope of the Lokbatan mud flow shown in Fig. 1. There are four general features of the solution for distance traveled. First, there is a weak dependence on block height w for large w since in this limit the expression in square parentheses in equation (8) approaches a constant value of 2. Second, the distance traveled scales approximately as $(L/h)^2$ (see equation (8)) owing to the high lubrication pressures (equation (5)) that reduce V . Third, block density has a small effect on distance travelled except for blocks with heights w_0 that approach the flow thickness h_0 . Fourth, the distance traveled will scale with $\tan \theta \approx \theta$ for small θ .

There are several idealizations in our model for the distance travelled. Mud breccias need not be Newtonian and can be shear-thinning and may have a yield stress (e.g. Knappe et al., 2020). The viscosity of natural mud breccias, however, approaches a constant value at strain-rates that might characterize natural, dense flows (Menapace et al., 2019). Further, we have assumed that the gap under the block is uniform in thickness so that V is only a function of $h(t)$, L , $w(t)$ and θ . Variations in gap thickness break the symmetry of the pressure distribution and would require a torque balance to determine how V also varies with x . Last, we have treated the flow as a unidirectional flow, neglecting the influence of flow around the block and irregularities in surface topography. All these

approximations were made to allow us to identify the dominant underlying physics of lubrication pressures on block transport.

4. Discussion

Our field measurements document minimal diffuse degassing during Lokbatan dormancy. We also identify large blocks that appear to be fragments of older cones that have been displaced as much as 1 km from the main crater. Here we address the significance of those observations for the frequency and violence of the eruptions. We use the model from the previous section to interpret the origin of the large blocks.

4.1. A self-sealing system

MV eruptions are short-duration events of fast overpressure release culminating with the extrusion of large volumes of fluids and mud breccia at the surface. These spectacular phenomena are separated by periods of quiescence. The length of this dormancy is related to the time required by the system to generate new overpressure essential to breach the seal that formed in the upper part of the conduit (or region of diffuse degassing) after each eruption. This overpressure is commonly generated by the migration of hydrocarbons from source rocks or shallower reservoirs (Mazzini, 2009). Continuous generation of hydrocarbons at depth and their migration often manifest at the surface as active pools, salsa lakes, and gryphons (Mazzini and Etiope, 2017). Dashgil MV (Azerbaijan) is a classic example where all these features (defined as macroseepages) are nicely displayed (Mazzini et al., 2009; Kopf et al., 2010). In addition to these obvious fluid degassing expressions, the release of gas at the surface of MVs also occurs through invisible and diffuse exhalation. This type of emission is called miniseepage (Etiope et al., 2011). It typically occurs over vast areas of the MV surface and often represents an output that is higher than the integrated sum from the visible macroseepage features (see Mazzini and Etiope, 2017 and references therein for detailed definitions and methods of measurements). It is difficult to correlate the effect of these combined surface degassing processes, operating during dormancy, and the generation of new overpressure required to trigger a new eruption event. Nevertheless these observations are essential to investigate the mechanisms controlling the type of MV activity (Mazzini and Etiope, 2017).

We propose that the intense eruptive activity of Lokbatan MV is related to the fast recharge of overpressure in the subsurface due to the efficient self-sealing characteristics of the system. We hypothesize that the feeder channel is plugged with mud breccia

at depth after the explosive eruptions. It should also be noted that significant hydrocarbon accumulations are present in reservoirs below Lokbatan MV (mostly located between 500–1500 m depth) and dozens of oil production wells operate around the crater (Feyzullayev et al., 2020). Despite the well-developed petroleum system in the Lokbatan area, the presence of gryphons, pools, or any other obvious enduring macroseepage features has never been reported, and observed during our field campaigns and the numerous surveys routinely completed by the oil company (SOCAR), by the Oil and Gas Institute of Azerbaijan, or by the Institute of Geology and Geophysics of the Azerbaijan National Academy of Sciences. In addition, during our 2005 and 2006 campaigns, Lokbatan MV was investigated with a Drager Pac Ex2 Methane sniffer (lower detection limit of 0.1%) and no evidence of methane seepage was observed throughout the surface of the structure. Only one small new-born isolated gryphon with negligible emissions (Fig. 3E, Table 2) was observed during the 2019 campaign. Although long-term monitoring of diffused miniseepage using a network of accumulation chambers (e.g. Cardellini et al., 2003b) would strengthen our observations, the collected data are consistently indicating very low gas emissions at Lokbatan MV. These observations are also consistent with our extensive survey, completed with more sensitive instruments, that also reveals limited CH₄ and CO₂ emissions (45 and 391.5 tonnes km⁻² yr⁻¹ respectively) present throughout the investigated area. The fluxes reported herein are significantly lower than those reported for most of the investigated MVs worldwide including some that are much smaller in size (Tables 1–2). These structures record much lower rates of eruptions compared to Lokbatan MV but have total emission factors up to 3 orders of magnitude higher.

Therefore our new data substantiate the Mazzini and Etiope (2017) suggestion that the recorded high rate of eruptions could be related to the ability of the volcano to seal off the overpressure generated by migrating hydrocarbons during periods of dormancy. This mechanism may explain the many frequent and violent events reported in the historical catalogues. This would also be in agreement with the discharge of copious amounts of mud breccia that characterize the Lokbatan MV. We argue that the documented explosive blowouts are capable of breaching portions of the crater and that the large volumes of erupted mud breccia become an efficient carrier for the huge cone fragments.

Additional support for the hypothesis that internal pressurization from self-sealing is the primary cause for the Lokbatan violent eruptions is provided by the lack of clear correlation between eruptions and either oil production or moderate to large regional earthquakes.

It has long been noted that moderate local and large regional earthquakes can trigger MV eruptions, including those in Azerbaijan (Mellors et al., 2007; Bonini et al., 2016). However, since eruptions may be triggered when a volcanic system is in a critical or metastable state, the correlation between these earthquakes and eruptions is not always unambiguous. Of the 25 Lokbatan eruptions since 1829 for which eruption dates are known, we could identify 4 eruptions with moderate M>5 earthquakes within the previous 12 months. We used earthquakes tabulated by Mellors et al. (2007) for the period before the 2001 eruption and the US Geological Survey catalogue for the period before eruptions in 2010, 2012 and 2017. The 1829 eruption occurred 149 days after a M5.7 event 59 km away; the 1990 eruption occurred 257 days after a M6.5 event 215 km away; the 2012 eruption occurred 40 days after a M6.4 event 179 km away. Mellors et al. (2007) report 6 earthquakes with larger ground motion intensity at Lokbatan that were not followed by an eruption within a year. The one exception is the 2001 eruption, that occurred 334 days after a M6.2 event only 46 km away; this particular earthquake-eruption pair is sometimes cited as an example of an earthquake-triggered eruption (Bonini et

al., 2016). There is no compelling evidence that earthquakes affect more than one, at most, Lokbatan eruption and this one example requires a process leading to a delayed eruption (by about 20% of the typical inter-eruption time). There were no Lokbatan eruptions within days to weeks of earthquakes with magnitudes similar to those that triggered MV eruptions elsewhere.

The immediate surroundings of the MV crater host a dense field of oil wells. Feyzullayev et al. (2020) identify no systematic relationship between eruptions and hydrocarbon production from wells tapping from productive horizons at depths ranging between 410 and 3600 m. This is consistent with the mud volcano source being pressurized at greater depths. In some instances the authors document an increase in hydrocarbon production after eruptive events. This aspect strengthens the hypothesis suggested by Mazzini and Etiope (2017), implying that the MV conduit and the hydrocarbon deposits are 1) either not connected (i.e., the overpressure in the conduit and the extruded fine-grained sediments compartmentalize the two systems), or 2) that during the eruption deeper seated mechanisms and fluids are predominant. This aspect is also supported by gas analyses from ephemeral seepage sites at Lokbatan MV. Results revealed the gas to be methane-dominated with minor amounts of ethane and propane indicating a thermogenic origin with C₁/C₂₊ ranging between 7–24 and δ¹³C-CH₄ ~-46‰ (Faber et al., 2015). This signature is similar to that reported from several other reservoirs sampled in Azerbaijan (e.g., Katz et al., 2002; Mazzini et al., 2009) or from localities where deep and rapidly rising methane has been inferred (e.g. Mazzini and Etiope, 2017 and refs therein). The Lokbatan MV gas signature suggests that, in contrast to the majority of the dormant MVs worldwide (Mazzini and Etiope, 2017), methane does not fractionate during the rapid migration process.

4.2. Large blocks rafting

The origin of large blocks on the flanks of MVs provides insights into the transport of mud breccia and the collapse of MV edifices. Roberts et al. (2011) adopt and refine the Planke et al. (2006) mud chamber collapse model and argue that the depression framing the long mud breccia flow at Lokbatan MV is related to thin-skinned sector collapse triggered by subsurface deflation that occurs after the eruptive events. The authors corroborate their hypothesis by proposing that the large blocks described herein are the evidence of debris avalanche deposits from the flank of the volcanic edifice. These events are suggested to be possibly related to sector collapse of the volcano at the end of the full eruption cycle of the 1935 eruption. Although the narrative description of this specific eruption can be interpreted as suggestive of a debris avalanche, photo documentations show that the megablocks themselves were already in place before that year (Jakubov et al., 1971). In addition, such debris avalanche events have never been witnessed in the highly populated and visited area at Lokbatan where, moreover, continuous petroleum industry operations have been active since the early 1930s (Jakubov et al., 1971). Plough-like depressions, similar to those described at Lokbatan MV, are not unique and are also observed contouring mud breccia flows at numerous MVs. This common feature is observed at, e.g., Kotturdag, Bahar, Shongar, Durandag, Bozdag Gobi, Airanteken, Dashmardan, Kechaldag, and other MVs (e.g. Jakubov et al., 1971; Aliyev et al., 2015; Mazzini and Etiope, 2017) where the mud flows extend for hundreds of meters and, particularly proximal to the crater, are bordered by steep walls several meters in height. If all these similar features were caused by mud chamber deflations (e.g. Roberts et al., 2011) this would imply that many MVs have a subsurface elongated chamber and that the mud flow direction is controlled by subsurface structures such as the anticline axes. Although this

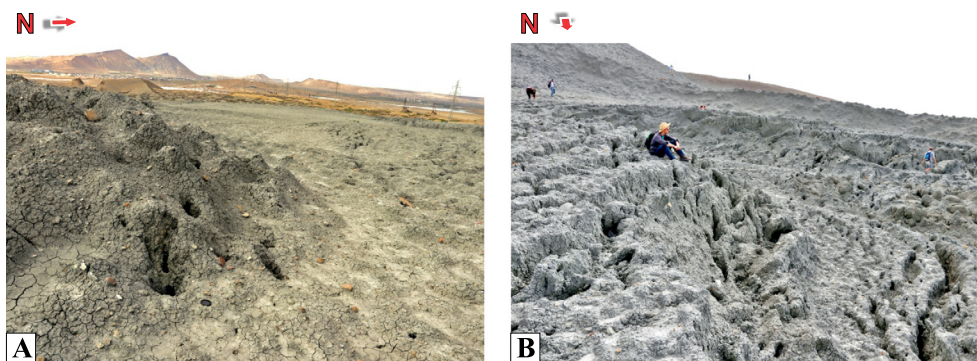


Fig. 8. Features at Lokbatan MV. (A) degassing conduits in mud breccia deposits indicating the fast degassing of fluid-rich sediment. Note that no evidence of ongoing seepage was observed at these sites during the survey periods. (B) Deflation features along the mud breccia flow.

may be sometimes the case, the same rule cannot be always applied.

We cannot rule out that some of the observed subvertical walls may be related to a potential faulting at the crest of the anticline upon which Lokbatan resides. We suggest instead an alternative mechanism that may explain the origin of observed depressions hosting the large-scale mud breccia flows. We hypothesize that during the eruptions, the large volumes of discharged viscous mud breccia have a ploughing effect on the flanks of the volcanoes. This bulldozing effect is prominent in the area closer to the crater, where the erupted mud is more confined, and becomes less effective moving downslope along the flanks. It is also important to note that the erupted mud is typically fluids-rich, containing large amounts of gas (the main process driving the eruption dynamics) and water. These fluids rapidly degas and evaporate during and immediately after the eruption, resulting in significant volume loss throughout the mud breccia tongue. This deflation effect can be clearly observed in the field at various MVs in the form of degassing cavities and conduits, desiccation patterns, and deflation features throughout the flows (Fig. 8A–B). This type of scenario is consistent with the records available from the 1887 Lokbatan winter eruption when witnesses described that “very stiff mud breccia flows (at least 2 m thick) were erupted forming a long tongue with a hummocky surface morphology” (Jakubov et al., 1971). The authors also report that during this eruption huge blocks were observed to have been transported, floating over the mud breccia flow. Similarly, lava flows that emerge from volcanic scoria cones are able to raft large blocks long distances (e.g., Németh et al., 2011; Valentine et al., 2017; Younger et al., 2019). We argue that a similar scenario occurred at Lokbatan MV where the violence of the eruptions enabled disruption or other disaggregation of the cones surrounding the active vent.

We now use our model to interpret the origin of the rafted blocks observed at the Lokbatan flow shown in Figs. 1 and 2. Flow thicknesses h_0 are a couple meters, the blocks have a thickness w_0 of many meters, and their lateral dimensions L are tens of meters to almost 100 m. w_0/h_0 is thus large enough to not influence transport distance (Fig. 7a). L/h_0 is between about 10 and 40, so we expect transport distances d/h_0 of approximately $50\text{--}10^3$ on the 6 degree slope of the Lokbatan MV. For flow thicknesses of 2 m, this implies transport from 100 m to 2 km, consistent with the distances to which blocks have been moved.

4.3. Implications for other MVs

Although the mud breccia blocks identified at Lokbatan MV are exceptionally large, similar features are present at other MVs. For example, Shongar MV, located a dozen kilometres to the NW, also displays large mud breccia blocks scattered along the main mud breccia flow (Fig. 9A–B). Large positive structures located on the

flanks or at the foot of other large MVs have been interpreted as eroded mud cones representing extinct satellite seepage sites. This interpretation may still be correct. Our findings, however, suggest that these features could also originate as large mud breccia blocks transported during eruptive events. Field observations may reveal if these represent rafted blocks. These would have a characteristic internal structure of thick sub-parallel mud breccia flows with distinct inner bedding. In contrast our observations show that dead satellite seepage sites (e.g., large gryphons) are characterized by thin laminated and concentric structures. In several instances is also possible to recognize remnants of a central feeder conduit that would not be present for blocks transported from other sites on the MV.

Large block-like features have also been imaged on multibeam and side-scan sonar data around the craters of offshore MVs. For example, pioneering 1980-90s sidescan sonar investigations from Black and Mediterranean seas interpreted these types of features as huge mud breccia clasts or as enigmatic features difficult to explain (e.g. Hieke et al., 1996; Ivanov et al., 1996). High-resolution bathymetry data may help to shed light on the origin of these features. Our novel megablock transport model opens new interpretations of mud eruption dynamics based on preserved structures. Similarly this different interpretation scenario may also lead to revisions of the inferred plumbing system of several MVs where, e.g., focused fluid migration may in fact occur exclusively at the crater site rather than diverging radially at several localities resulting in erroneously interpreted gryphons or mud cones.

5. Conclusions

- 1) Despite its frequent, large volume eruptions, Lokbatan mud volcano has minimal degassing when not erupting compared to other mud volcanoes. We propose that Lokbatan effectively seals subsurface conduits after eruptions, allowing pressure to recharge more rapidly than at other mud volcanoes – leading to more frequent, more energetic, and larger eruptions. The correlation between the ability of an active system to self-seal and the energy of eruptions, may be universal for mud volcanoes. Continued long-term monitoring of microseepage gas flux can confirm this hypothesis.
- 2) These powerful eruptions are also able to break apart mud breccia cones and transport blocks with the mud breccia flows. Using a lubrication theory model, we show that the distance blocks travel is controlled largely by their lateral dimension compared to the thickness of the underlying flow, making it possible for larger blocks to be transported further than smaller ones.
- 3) We postulate a bulldozing (ploughing) effect of great volume of viscous mud breccia on the upper parts of MV edifice when

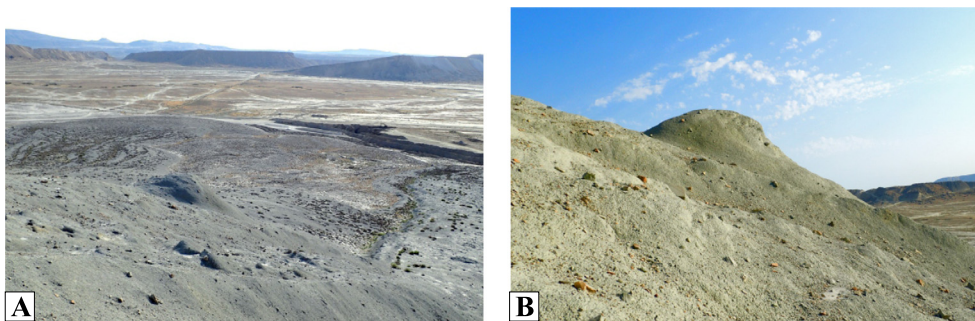


Fig. 9. (A–B) Examples of large blocks observed at Shongar MV. These blocks may reach the size of $5 \times 20 \times 20$ m.

mud flow outspreads from elevated craters during high-energy eruptions.

- 4) Based on the available records of eruption witnesses (see reports in Jakubov et al., 1971), we suggest that the origin of the spectacular Lokbatan megablocks is connected with the 1887 eruption, since the descriptions of this event report that large blocks were transported along with the erupting mud breccia flow.

CRediT authorship contribution statement

AM and **GA** designed and organized the study. **AM**, **MM** and **GA** organized the structure of the manuscript and the various phases of writing-reviewing and editing. **MM** performed the calculations for the lubrication model. **AS** performed the flux measurements and data elaboration. **AM** secured the funding for the study. All authors contributed to final editing of the manuscript and during the field expeditions.

Declaration of competing interest

The authors declare that they have no known competing financial interests or personal relationships that could have appeared to influence the work reported in this paper.

Acknowledgements

This study was carried out with the financial support of the Research Council of Norway (NFR) through the HOTMUD project number 288299 and its Centers of Excellence funding scheme, project number 223272 (CEED). **MM** is supported by the US National Science Foundation EAR 1615203. The editor and two anonymous reviewers are thanked for their useful comments and corrections that greatly improved the manuscript.

References

- Aliyev, A., Guliyev, F., Dadashev, F.G., Rahmannov, R.R., 2015. Atlas of the World Mud Volcanoes. Nafta-Press. ISBN 978-9952-437-60-7.
- Aliyev, A., Guliyev, I.S., Belov, I.S., 2002. Catalogue of Recorded Eruptions of Mud Volcanoes of Azerbaijan. Nafta Press, Baku. 87 p.
- Baciu, C., Ionescu, A., Etiope, G., 2018. Hydrocarbon seeps in Romania: gas origin and release to the atmosphere. *Mar. Pet. Geol.* 89, 130–143.
- Bonini, M., 2012. Mud volcanoes: indicators of stress orientation and tectonic controls. *Earth-Sci. Rev.* 115.
- Bonini, M., Rudolph, M.L., Manga, M., 2016. Long- and short-term triggering and modulation of mud volcano eruptions by earthquakes. *Tectonophysics* 672–673, 190–211.
- Cardellini, C., Chiodini, G., Frondini, F., 2003a. Application of stochastic simulation to CO₂ flux from soil: mapping and quantification of gas release. *J. Geophys. Res.* 108 (B9), 2425–2438.
- Cardellini, C., Chiodini, G., Frondini, F., Granieri, D., Lewicki, J., Peruzzi, L., 2003b. Accumulation chamber measurements of methane fluxes: application to volcanic-geothermal areas and landfills. *Appl. Geochem.* 18 (1), 45–54.
- Chiodini, G., Frondini, F., 2001. Carbon dioxide degassing from the Albani Hills volcanic region, Central Italy. *Chem. Geol.* 177, 67–83.

- Etiope, G., Baciu, C., Caracausi, A., Italiano, F., Cosma, C., 2004a. Gas flux to the atmosphere from mud volcanoes in eastern Romania. *Terra Nova* 16 (4), 179–184.
- Etiope, G., Ciotoli, G., Schwietzke, S., Schoell, M., 2019. Gridded maps of geological methane emissions and their isotopic signature. *Earth Syst. Sci. Data* 11 (1), 1–22.
- Etiope, G., Feizullayev, A.A., Baciu, C.L., Milkov, A., 2004b. Methane emission from mud volcanoes in eastern Azerbaijan. *Geology* 32 (6), 465–468.
- Etiope, G., Martinelli, G., Caracausi, A., Italiano, F., 2007. Methane seeps and mud volcanoes in Italy: gas origin, fractionation and emission to the atmosphere. *Geophys. Res. Lett.* 34 (14), L14303.
- Etiope, G., Nakada, R., Tanaka, K., Yoshida, N., 2011. Gas seepage from Tokamachi mud volcanoes, onshore Niigata Basin (Japan): origin, post-genetic alterations and CH₄–CO₂ fluxes. *Appl. Geochem.* 26 (3), 348–359.
- Faber, E., Schmidt, M., Feizullayev, A., 2015. Geochemical hydrocarbon exploration - insights from stable isotope models. *Oil Gas Eur. Mag.* 41, 93–98.
- Feizullayev, A., Lerche, I., Gojayev, A., 2020. About the Impact of Mud Volcano Eruptions and Earthquake on Petroleum Production Rates (South Caspian Basin). *Int. J. Eng. Res. Technol.* 09 (08).
- Frunzeti, N., Baciu, C., Etiope, G., Pfanz, H., 2012. Geogenic emission of methane and carbon dioxide at Beciu mud volcano (Berca-Arbanasi hydrocarbon-bearing structure, Eastern Carpathians, Romania). *Carpath. J. Earth. Environ. Sci.* 7, 159–166.
- Hieke, W., Werner, F., Schenke, H.W., 1996. Geomorphological study of an area with mud diapirs South of Crete (Mediterranean Ridge). *Mar. Geol.* 132 (1), 63–93.
- Hong, W.-L., Etiope, G., Yang, T.F., Chang, P.-Y., 2013. Methane flux from miniseepage in mud volcanoes of SW Taiwan: comparison with the data from Italy, Romania, and Azerbaijan. *J. Asian Earth Sci.* 65 (C), 3–12.
- Hutchinson, G.L., Livingston, G.P., Healy, R.W., Striegl, R.G., 2000. Chamber measurement of surface-atmosphere trace gas exchange: numerical evaluation of dependence on soil, interfacial layer, and source/sink properties. *J. Geophys. Res., Atmos.* 105 (D7), 8865–8875.
- Ivanov, M.K., Limonov, A.F., van Weering, T.C.E., 1996. Comparative characteristics of the Black Sea and Mediterranean Ridge mud volcanoes. *Mar. Geol.* 132 (1–4), 253–271.
- Jakubov, A.A., AliZade, A.A., Zeinalov, M.M., 1971. Mud Volcanoes of the Azerbaijan SSR: Atlas (in Russian). Azerbaijan Academy of Sciences, Baku.
- Katz, B.J., Narimanov, A., Huseinzadeh, R., 2002. Significance of microbial processes in gases of the South Caspian basin. *Mar. Pet. Geol.* 19 (6), 783–796.
- Knappe, E., Manga, M., Le Friant, A., 2020. Rheology of natural sediments and its influence on the settling of dropstones in marine hemipelagic sediment. *Earth Space Sci.* 7 (3), e2019EA000876.
- Kopf, A., Delisle, G., Faber, E., Panahi, B., Aliyev, C.S., Guliyev, I., 2010. Long-term in situ monitoring at Dashgil mud volcano, Azerbaijan: a link between seismicity, pore-pressure transients and methane emission. *Int. J. Earth Sci.* 99 (1), 227–240.
- Mazzini, A., 2009. Mud volcanism: processes and implications. *Mar. Pet. Geol.* 26 (9), 1677–1680.
- Mazzini, A., Etiope, G., 2017. Mud volcanism: an updated review. *Earth-Sci. Rev.* 168, 81–112.
- Mazzini, A., Svensen, H., Planke, S., Guliyev, I., Akhmanov, G.G., Fallik, T., Banks, D., 2009. When mud volcanoes sleep: insight from seep geochemistry at the Dashgil mud volcano, Azerbaijan. *Mar. Pet. Geol.* 26 (9), 1704–1715.
- Mellors, R., Kilb, D., Aliyev, A., Gasanov, A., Yetirmishli, G., 2007. Correlations between earthquakes and large mud volcano eruptions. *J. Geophys. Res.* 112, B04304.
- Menapace, W., Tangunan, D., Maas, M., Williams, T., Kopf, A., 2019. Rheology and biostratigraphy of the Mariana Serpentine Muds Unravel Mud Volcano evolution. *J. Geophys. Res., Solid Earth* 124 (11), 10752–10776.
- Németh, K., Rizzo, C., Nullo, F., Kereszturi, G., 2011. The role of collapsing and cone rafting on eruption style changes and final cone morphology: Los Morados scoria cone, Mendoza, Argentina. *Cent. Eur. J. Geosci.* 3 (2), 102–118.
- Planke, S., Mazzini, A., Svensen, H., Akhmanov, G.G., Malthe-Sorensen, A., 2006. Mud Volcanoes in Azerbaijan. In: Implications for Sediment and Fluid Migration in Active Piercement Structures.

- Roberts, K.S., Stewart, S.A., Davies, R.J., Evans, R.J., 2011. Sector collapse of mud volcanoes, Azerbaijan (Author abstract) (Report). *J. Geol. Soc.* 168 (1), 49.
- Sciarra, A., Cantucci, B., Ricci, T., Tomonaga, Y., Mazzini, A., 2019. Geochemical characterization of the Nirano mud volcano, Italy. *Appl. Geochem.* 102, 77–87.
- Sibson, R., 1981. A brief description of natural neighbour interpolation (chapter 2). In: Barnett, V. (Ed.), *Interpreting Multivariate Data*. John Wiley, Chichester, UK, pp. 21–36.
- Sinclair, A.J., 1974. Selection of threshold values in geochemical data using probability graphs. *J. Geochem. Explor.* 3, 129–149.
- Sinclair, A.J., 1991. A fundamental approach to threshold estimation in exploration geochemistry: probability plots revisited. *J. Geochem. Explor.* 41, 1–22.
- Spulber, L., Etiopie, G., Baciu, C., Maloş, C., Vlad, Ş.N., 2010. Methane emission from natural gas seeps and mud volcanoes in Transylvania (Romania). *Geofluids* 10 (4), 463–475.
- Sumgait, 2016. January 5, [Video File]. Retrieved from <https://www.youtube.com/watch?v=xcecyOgZmrA>.
- Valentine, G.A., Cortés, J.A., Widom, E., Smith, E.I., Rasoazanamparany, C., Johnsen, R., Briner, J.P., Harp, A.G., Turrin, B., 2017. Lunar Crater volcanic field (Reveille and Pancake Ranges, Basin and Range Province, Nevada, USA). *Geosphere* 13 (2), 391–438.
- Younger, Z.P., Valentine, G.A., Gregg, T.K.P., 2019. 'A' lava emplacement and the significance of rafted pyroclastic material: Marcath volcano (Nevada, USA) (Report). *Bull. Volcanol.* 81 (9), 1.
- Zheng, G., Ma, X., Guo, Z., Hilton, D.R., Xu, W., Liang, S., Fan, Q., Chen, W., 2017. Gas geochemistry and methane emission from Dushanzi mud volcanoes in the southern Junggar Basin, NW China. *J. Asian Earth Sci.* 149, 184–190.